



Research paper

Buckling resistance of the wall of a steel grain silo

Jakub Marcinowski¹, Volodymyr Sakharov²

Abstract: The walls of steel grain silos are susceptible to buckling. The reason for this undesirable phenomenon is the vertical impact of grain stored in the silo on the walls, most often made of corrugated sheet metal with horizontal corrugations. External, vertical stiffeners make a wall strengthened and together with corrugated sheet metals create orthogonal shell structure. The procedures included in the applicable standards make it possible to estimate the buckling load capacity of the wall of a silo constructed in this way. The paper presents an example of the analysis of the buckling load capacity of the wall of a steel silo with a capacity of 700 m³. Two of the methods recommended in applicable standards were used. Numerical simulations were also performed to determine the critical level of load intensity. The analyses carried out allowed conclusions to be drawn regarding the buckling load capacity of the wall of the analysed silo.

Keywords: analytical calculations, buckling resistance, corrugated steel sheet, numerical simulations, steel silo, wall stiffeners

¹Prof., DSc., PhD., Eng., University of Zielona Gora, Poland, Institute of Civil Engineering, Szafrana 1, 65-516 Zielona Gora, Poland, e-mail: j.marcinowski@ib.uz.zgora.pl, ORCID: 0000-0001-6834-0843

²DSc., PhD., Eng., University of Zielona Gora, Poland, Institute of Civil Engineering, Szafrana 1, 65-516 Zielona Gora, Poland, e-mail: v.sakharov@ib.uz.zgora.pl, ORCID: 0000-0002-9381-3283

1. Introduction

Steel grain silos belong to the group of very light and slender structures. The pressure of the grain stored inside them only seemingly stabilizes the walls by causing circumferential stretching. In addition to the normal component to the wall surface, there is also a tangential component causing compression of the wall in the meridional direction. These forces can cause a loss of stability of the wall, often leading to the complete destruction of the silo.

The growing market demand for this type of storage facility and the competitiveness of offers from domestic and foreign manufacturers result in structural solutions leading to the minimization of their weight. Both the thickness of shell plates (steel sheets) and the thickness of plates from which cold-formed sections of stiffeners reinforcing the silo wall from the outside are minimized. Such an approach, which is not supported by detailed analyses confirming the correctness of the design solutions used, can result in failure conditions.

The relatively high frequency of failures of steel silos has made these structures the object of interest for many domestic and foreign authors. The list of publications cites works from the last 10 years [1–14]. Most of them were written based on the silo failures that occurred.

In the presented work, analyses regarding the buckling capacity of the wall of a silo with a capacity of 700 m³ and a total height of 24 meters are included. These analyses were carried out using standard procedures contained in norms [15] and [16]. Due to significantly divergent results, numerical simulations were also performed to determine the load level causing the loss of wall stability. The results of the numerical simulations, as the most reliable, were the basis for formulating conclusions regarding the buckling resistance of the wall of the analyzed silo.

2. Description of the silo

The view and basic dimensions of the analyzed silo are shown in Fig. 1. The cylindrical part of the silo has a height of 17,104 meters and consists of 15 strakes, each 1140 mm in height. The thickness of the sheets of the two bottom strakes is 1.5 mm (the steel sheet just above the hopper ring) and 1.2 mm (next strake). The steel sheets of the remaining strakes have a constant thickness of $t = 0.8$ mm. The sheets are connected with M10 bolts of grade 8.8. The diameter of the holes is $\phi = 12$ mm.

The hopper, made of smooth sheets, has a 45-degree slope, and its ring rests on 18 columns, each 5.40 meters long, made from HEB120 sections. These columns are extended by 18 stiffeners that reinforce the cylindrical part of the silo (Fig. 1).

The silo walls' sheets have been externally reinforced with cold-formed sections (stiffeners) with a profile shaped like an inverted channel. The circumferential spacing of the stiffeners is 1200 mm. The connection of the stiffeners to the corrugated wall sheets was made using bolts.

The silo roof has the shape of a truncated cone with a slope of 30 degrees. The roof sheeting rests on a framework made of cold-formed sections.

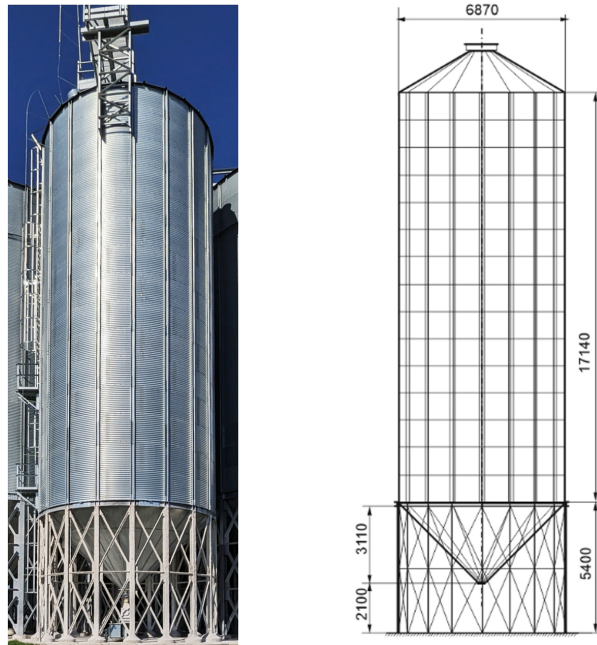


Fig. 1. View of the silo and its overall dimensions

3. Structural calculations of the silo wall

3.1. Load summary

The method for loading the silo walls is defined by standard [17]. The considered silo has a capacity of 700 m³. According to the classification provided in section 2.5 of standard [17], we are dealing with an AAC2 action assessment class silo.

The ratio of the height of the cylindrical part to the diameter of the silo is:

$$(3.1) \quad \frac{h_c}{d_c} = \frac{17.14}{6.87} = 2.53 > 2$$

According to the classification provided in section 5.1 of PN-EN 1991-4:2006 [17], this is classified as a slender silo.

Loads in the filled and discharging states were determined based on the provisions of sections 5.2.1.1 and 5.2.2.1 of standard [17].

The values of horizontal pressure p_{hf} , surface friction against the wall p_{wf} , and vertical pressure p_{vf} at any depth z upon filling or during storage were determined using formulas (5.1) to (5.6) from standard [17].

From Table E.1 of standard [17], we adopted: $\gamma = \gamma_u = 9 \text{ kN/m}^3$ – the characteristic value of the bulk density of wheat (upper value).

According to Table 4.1 of standard [17], we are dealing with a D4 category wall case. The friction coefficient for such a wall is determined using formula (D.1) from Appendix D of standard [17]:

$$(3.2) \quad \mu_{\text{eff}} = (1 - a_w) \cdot \text{tg } \phi_i + a_w \mu_w$$

where:

ϕ_i – is the internal friction angle of the stored material,

μ_w – is the friction coefficient against flat sheet metal (D2 wall case),

a_w – is a coefficient determined as explained in the standard.

Based on data from Table E.1 of standard [17], the friction coefficient (lower value) is:

$$(3.3) \quad \mu_w = \frac{\mu_{wm}}{a_\mu} = \frac{0.38}{1.16} = 0.3276$$

For wheat (Table E.1 of standard [17]), the internal friction angle (lower value) is:

$$(3.4) \quad \phi_i = \frac{\phi_{im}}{a_\phi} = \frac{30}{1.12} = 26.79$$

For corrugated sheet metal, it can be assumed (see section D.2 (3) of standard [17]): $a_w = 0.2$. The effective friction coefficient is:

$$(3.5) \quad \mu_{\text{eff}} = (1 - a_w) \cdot \text{tg } \phi_i + a_w \mu_w = (1 - 0.2) \cdot \text{tg } 26.79 + 0.2 \cdot 0.3276 = 0.469$$

The lateral pressure ratio value was determined based on data from Table E.1 of standard [17] (upper value):

$$(3.6) \quad K = K_m \cdot a_K = 0.54 \cdot 1.11 = 0.599$$

Geometric dimensions used in the calculations:

$$(3.7) \quad A = \pi \frac{d_c^2}{4} = \pi \frac{6.87^2}{4} = 37.07 \text{ m}^2$$

$$U = \pi d_c = \pi \cdot 6.87 = 21.583 \text{ m}$$

where:

A – is the cross-sectional area of the silo,

U – is the circumference of the silo cross-section.

The level of the equivalent surface was determined based on the internal friction angle ϕ_i and the roof slope angle. The equivalent surface level of the grain is located 44 cm above the upper edge of the cylindrical part of the silo.

The loads in the discharging state were obtained by multiplying the load values for the filled state by the increase factors specified in standard [17]. For slender silos meeting the AAC2 action assessment class criteria, these factors are (see Section 5.2.2.1 of standard [14]):

– for horizontal loads: $C_h = 1.15$,

– for tangential loads acting on the wall: $C_w = 1.10$.

Table 1 presents the values of forces in the stiffeners reinforcing the silo walls. The table provides characteristic values for the filled and discharging states. The variation of these forces along the height of the silo is shown in Fig. 2.

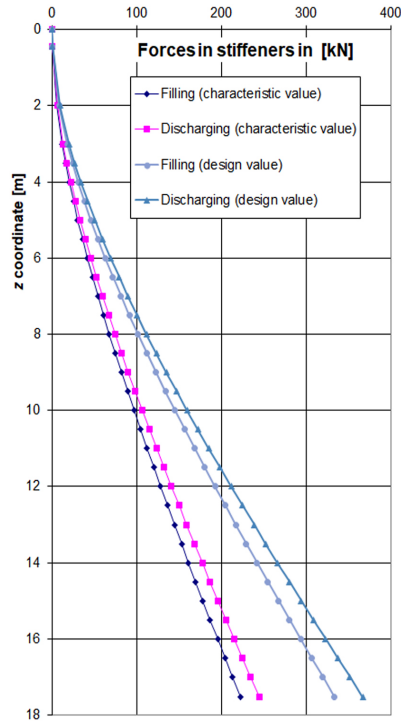


Fig. 2. Forces in wall stiffeners

Table 1. Summary of forces in stiffeners

z [m]	p_{wf} [kN/m ²]	$N_{f, ch}$ [kN]	$N_{d, ch}$ [kN]
0	0.00	0.00	0.00
0.44	1.12	0.30	0.33
2.00	4.49	5.69	6.26
3.00	6.22	12.15	13.36
4.00	7.68	20.51	22.56
5.00	8.91	30.47	33.52
6.00	9.94	41.79	45.97
7.00	10.81	54.25	59.67
8.00	11.54	67.66	74.43
9.00	12.16	81.89	90.07

Table continued on the next page

Table continued from the previous page

z [m]	p_{wf} [kN/m ²]	$N_{f, ch}$ [kN]	$N_{d, ch}$ [kN]
10.00	12.68	96.79	106.47
11.00	13.12	112.26	123.49
12.00	13.49	128.22	141.04
13.00	13.80	144.59	159.05
14.00	14.06	161.29	177.42
14.50	14.18	169.76	186.73
15.00	14.28	178.29	196.12
15.50	14.38	186.88	205.57
16.00	14.47	195.53	215.08
16.50	14.55	204.23	224.65
17.00	14.62	212.97	234.27
17.54	14.70	222.43	244.67

The following notations are used in Table 1:

p_{wf} – tangential pressure on the wall in the filled state (characteristic value),

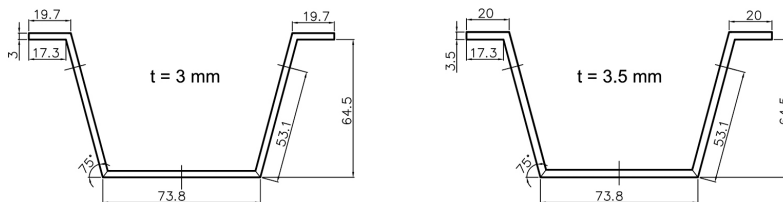
N_f – force in the wall column in the filled state (f – filling),

N_d – force in the wall column in the discharging state (d – discharging),

$()_{ch}$ – characteristic value.

3.2. Section resistance of silo wall reinforcement stiffeners

In the lower section of the cylindrical part of the silo, there is a first section of reinforcing stiffener with a thickness $t = 3.5$ mm. The next stiffener segment (the next section) has a thickness of $t = 3$ mm (see Fig. 3). The stiffeners were made from a 237 mm wide flat bar using a cold forming process. HX500LAD steel was used, for which $f_y = 500$ MPa. The cross-sections of the stiffeners are 8.30 cm² and 71.1 cm², and their sectional compression resistance is equal to 415 kN and 356 kN for $t = 3.5$ mm and $t = 3.0$ mm, respectively. The compressive forces of the lower N_{Ed} stiffener sections do not exceed 245 kN (cf. Table 1). The compression resistance of the stiffener sections also checked for the higher sections of the silo wall proved to be sufficient.

Fig. 3. Cross-sections of stiffeners $t = 3$ mm and $t = 3.5$ mm

The standards [15] and its annex [16] provide two methods for estimating the buckling capacity of stiffeners reinforcing the cylindrical wall of a silo. The first method involves replacing the system of a corrugated sheet wall and external stiffeners, plus potentially circumferential rings, with an equivalent cylindrical shell with orthotropic characteristics.

Tangential vertical forces $n_{x,Ed}$ from the friction of the grain against the wall surface can cause a loss of stability, potentially leading to the complete destruction of the silo. The load-bearing criterion is formulated as follows (see [15] formula (5.63)):

$$(3.8) \quad n_{x,Ed} \leq n_{x,Rd}$$

where: $n_{x,Ed}$ is the meridional force, and $n_{x,Rd}$ is the buckling capacity of the orthotropic shell. This value is defined by formula (5.69) [15]:

$$(3.9) \quad n_{x,Rd} = \frac{\alpha_x n_{x,Rcr}}{\gamma_{M1}}$$

where: $\alpha_x = 0.8$ [15], $\gamma_{M1} = 1.1$ [15].

The method for verifying the buckling capacity of the silo wall under meridional compression is described in section 5.3.4.3.3 of the PN EN 1993-4-1 standard. The silo wall can be treated as an orthotropic shell provided that the circumferential spacing of the stiffeners does not exceed the value:

$$(3.10) \quad d_{s,max} = k_{d\theta} \left(\frac{r^2 D_y}{C_y} \right)^{0.25}$$

where: D_y – is the bending stiffness per unit width in the direction of the panel corrugation (steel sheet) with the thinnest sheet metal, C_y – is the membrane stiffness per unit width in the direction of the panel corrugation (steel sheet) with the thinnest sheet metal, and r is the radius of the cylindrical shell.

The recommended value of the coefficient $k_{d\theta} = 7.4$. With:

$$(3.11) \quad \begin{aligned} D_\theta &= D_y = 0.13 E t d^2 \\ C_\theta &= C_y = E t \left(1 + \frac{\pi^2 d^2}{4l^2} \right) \end{aligned}$$

according to formula (4.6) and (4.5) from [15] respectively. The parameters l , t , and d in these formulas are the wave parameters of the shell (wave length $l = 76$ mm, wave height $d = 14$ mm) and the sheet metal thickness $t = 0.8$ mm at the point of checking the buckling capacity.

For the considered silo:

$$(3.12) \quad d_{s,max} = k_{d\theta} \left(\frac{r^2 D_y}{C_y} \right)^{0.25} = 955 \text{ mm}$$

The spacing of the stiffeners used in the silo $d = 1200$ mm exceeds this value. Despite not meeting this condition, the procedure from section 5.3.4.3.3 of the standard [15] was applied, treating the obtained results as an approximate assessment of the buckling capacity of the silo wall.

In the considered cross-sections of the silo (selected strakes), the critical value of the meridional force $n_{x,Rcr}$ was determined by minimizing the expression below concerning the critical number of circumferential waves j and the height of the buckling half-wave l_i of the silo shell. This pressure is determined by formula (5.65) of the standard [15]:

$$(3.13) \quad n_{x,Rcr} = \frac{1}{j^2 \omega^2} \left(A_1 + \frac{A_2}{A_3} \right)$$

where:

$$(3.14) \quad \begin{aligned} A_1 &= j^4 [\omega^4 C_{44} + 2\omega^2 (C_{45} + C_{66}) + C_{55}] + C_{22} + 2j^2 C_{25} \\ A_2 &= 2\omega^2 (C_{12} + C_{33}) (C_{22} + j^2 C_{25}) (C_{12} + j^2 \omega^2 C_{14}) \\ &\quad - (\omega^2 C_{11} + C_{33}) (C_{22} + j^2 C_{25})^2 - \omega^2 (C_{22} + \omega^2 C_{33}) (C_{12} + j^2 \omega^2 C_{14})^2 \\ A_3 &= (\omega^2 C_{11} + C_{33}) (C_{22} + C_{25} + \omega^2 C_{33}) - \omega^2 (C_{12} + C_{33})^2 \\ C_{11} &= C_\phi + \frac{EA_s}{d_s} \quad C_{22} = C_\theta + EA_r/d_r \\ C_{12} &= \nu \sqrt{C_\phi C_\theta} \quad C_{33} = C_{\phi\theta} \\ C_{14} &= \frac{e_s EA_s}{rd_s} \quad C_{25} = e_r EA_r/(rd_r) \\ C_{44} &= \frac{[D_\phi + \frac{EI_s}{d_s} + \frac{EA_s e_s^2}{d_s}]}{r^2} \quad C_{55} = \frac{[D_\theta + \frac{EI_r}{d_r} + \frac{EA_r e_r^2}{d_r}]}{r^2} \\ C_{45} &= \frac{\nu \sqrt{D_\phi D_\theta}}{r^2} \quad C_{66} = \frac{[D_{\phi\theta} + 0.5(\frac{GI_s}{d_s} + \frac{GI_r}{d_r})]}{r^2} \\ \omega &= \frac{\pi r}{jl_i} \end{aligned}$$

where:

l_i – is the length of the vertical half-wave corresponding to the potential buckling form; it should be selected to minimize values $n_{x,Rcr}$ according to (3.13),

A_s – is the cross-sectional area of the stringer stiffener,

I_s – is the moment of inertia of the vertical stiffener's cross-section relative to its own axis parallel to the circumference,

d_s – is the spacing of stringer stiffeners,

I_{ts} – is the uniform torsion constant of the stringer stiffener,

e_s – is the eccentricity of the stringer stiffener measured from the mid-surface of the shell,

A_r – is the cross-sectional area of the ring stiffener,

I_r – is the moment of inertia of the stiffening ring's cross-section relative to the vertical axis (circumferential bending),

d_r – is the distance between ring stiffeners,

I_{tr} – is the uniform torsion constant of the ring stiffener,

e_r – is the eccentricity of the stiffening ring measured from the mid-surface of the shell,

C_ϕ – is the sheeting stretching stiffness in the meridional direction (see Section 4.4 in standard [14]),

C_θ is the sheeting stretching stiffness in the circumferential direction (see Section 4.4 in standard [14]),

$C_{\phi\theta}$ – is the sheeting stretching stiffness in membrane shear (see section 4.4 in standard [14]),
 D_{ϕ} – is the sheeting flexural rigidity in the axial direction (see Section 4.4 in standard [14]),
 D_{θ} – is the sheeting flexural rigidity in the circumferential direction (see Section 4.4 in standard [14]),

D – is the sheeting twisting flexural rigidity in twisting (see Section 4.4 in standard [14]),
 r – is the radius of the cylindrical shell,

j – is the number of full waves around the circumference; it should be selected to minimize (3.13).

The design value of the meridional force causing buckling, i.e., the buckling capacity, is determined from formula (3.15):

$$(3.15) \quad n_{x,Rd} = \alpha_n \frac{n_{x,Rcr}}{\gamma_{M1}} = \frac{0.8}{1.1} n_{x,Rcr} = 0.727 n_{x,Rcr}$$

The buckling capacity of the silo wall was verified for data from the area of the third shell from the bottom. The calculation results are presented in Table 2 and Figure 4.

Table 2. Results of calculations

Radius of cylindrical part of silo: $r = 3435$ mm, steel sheet plate: $t = 0.8$ mm, $d = 14$ mm, $l = 76$ mm, $E = 210\,000$ MPa. stiffener thickness: $t_{st} = 3$ mm, $e_s = 36.83$ mm, $A_s = 723.5$ mm ² , $I_s = 45.85 \cdot 10^4$ mm ⁴ , $I_{ts} = 0.065 \cdot 10^4$ mm ⁴ , $C_{\phi} = 365.714$ N/mm, $C_{\theta} = 1.821 \cdot 10^5$ N/mm, $D_{\phi} = 9085$ Nmm ² /mm, $D_{\theta} = 4.281 \cdot 10^6$ Nmm ² /mm, $C_{\phi\theta} = 5.962 \cdot 10^4$ N/mm, $D_{\phi\theta} = 3735$ Nmm ² /mm.	For $j = 4$, $l_i = 17100$ mm, $n_{x,Rcr} = 491.81$ kN/m, (see Fig. 5).
--	--

The smallest value of $n_{x,Rcr}$ was obtained for $l_i = 17\,100$ mm, i.e. a buckling half-wave equal to the full height of the cylindrical part of the silo, and for $j = 4$, i.e. for 4 waves around the perimeter.

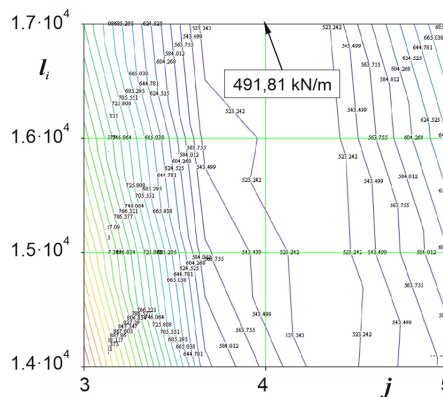


Fig. 4. Determination of the minimum of the function $n_{x,Rcr}(j, l_i)$

The bearing capacity of an orthotropic wall in the meridional direction is obtained from the formula (3.15):

$$(3.16) \quad n_{x,Rd} = 0.727n_{x,Rcr} = 0.727 \cdot 491.81 = 357.54 \text{ kN/m}$$

Each stiffener is subjected to a force $N_{x,Rd} = 357.54 \cdot 1.2 = 429.08 \text{ kN}$. This value is significantly higher than the compressive force in the stiffener at the considered section: $N_{Ed} = 205.57 \text{ kN}$ (discharge state, characteristic value; see Table 1, position for $z = 15.5 \text{ m}$). The standard buckling capacity criterion is therefore met under this condition.

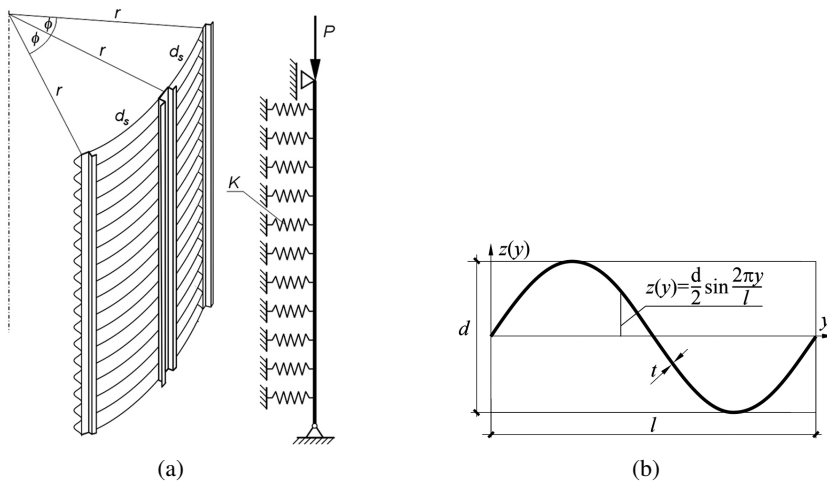


Fig. 5. Wall stiffener as a bar on an elastic foundation (a) and method of profiling the sheeting (b)

An alternative method for estimating the capacity of the wall stiffener is described in section 20 of the annex [16] to the standard [15]. This approach involves considering the stiffener as a compressed member resting on an elastic foundation and hinged at the ends (see Fig. 5a).

The stiffness parameter K depends on the material and geometry of the silo wall. It is determined according to formulas (5.74) to (5.76a) from [16], where the basic stiffness parameters of the corrugated sheet metal are defined as follows (see Fig. 5b):

$$(3.17) \quad C_y = \frac{EA_f}{l} \cong Et \left(1 + \frac{\pi^2 d^2}{4l^2} \right)$$

$$(3.18) \quad D_y = \frac{EJ_{fy}}{l} \cong \frac{1}{8} Et d^2 \left(1 + \frac{\pi^2 d^2}{8l^2} \right)$$

The formula for the stiffness parameter K is of the form (see formula (5.74) of [16]):

$$(3.19) \quad K = \frac{1}{r} \left\{ \frac{2C_y D_y - \sin^2 \phi}{v} \right\}$$

where:

$$(3.20) \quad \phi = \frac{d_s}{r}$$

$$(3.21) \quad v = fD_y + r^2C_y f + \phi \cos^2 \phi (\tan \phi + 2g)^2 - 2[2g^2 \sin 2\phi - 2g(\cos 2\phi - \cos \phi) - \sin \phi(\cos \phi - 1)]$$

$$(3.22) \quad g = \frac{r^2C_y[(1 - \cos \phi)(1 + 3 \cos \phi) - \phi \sin 2\phi] - D_y \sin^2 \phi}{D_y(2\phi + \sin 2\phi) + r^2C_y[2\phi(2 + \cos 2\phi) - 3 \sin 2\phi]}$$

$$(3.23) \quad f = \frac{1}{4} \{(4g^2 + 1)(2\phi + \sin 2\phi) + 4g(1 - \cos 2\phi) - 2 \sin 2\phi\}$$

In formula (3.22) for g , the corrections suggested in the paper [14] are included.

The effective length of the compression bar is calculated from the formula (5.72) in [16]:

$$(3.24) \quad L_e = \pi \left(\frac{EI_{sy}}{K} \right)^{1/4}$$

and from this the reduction factor χ of the flexural buckling resistance of the bar (stiffener) is determined using the procedure described in clause 6.3.1.3 of [18]. The buckling resistance $N_{b,Rd}$ obtained as a result of this procedure is compared with the force N_{Ed} occurring in the stiffener at the considered height of the silo wall.

Table 3. Calculations of buckling resistance of stiffeners

13th strake, plate $t = 0.8$ mm, stiffener $t_{st} = 3.0$ mm, $A_s = 7.235$ cm ² , $J_{sy} = 45.852$ cm ⁴ , $f_y = 500$ MPa, $K = 0.6036$ N/mm ² , $L_e = 198.5$ cm	$N_{b,Rd} = 152.64$ kN, $N_{Ed} = 205.57$ kN, exceeding 35%
14th strake, plate $t = 1.2$ mm, stiffener $t_{st} = 3.5$ mm, $A_s = 8.431$ cm ² , $J_{sy} = 53.425$ cm ⁴ , $f_y = 500$ MPa, $K = 0.9054$ N/mm ² , $L_e = 186.4$ cm	$N_{b,Rd} = 193.18$ kN, $N_{Ed} = 224.65$ kN, exceeding 16%
15th strake, plate $t = 1.5$ mm, stiffener $t_{st} = 3.5$ mm, $A_s = 8.431$ cm ² , $J_{sy} = 53.425$ cm ⁴ , $f_y = 500$ MPa, $K = 1.132$ N/mm ² , $L_e = 176.3$ cm	$N_{b,Rd} = 206.90$ kN, $N_{Ed} = 244.67$ kN, exceeding 18%

The results of the calculations for the three selected stiffener cross-sections (three bottom strakes) are presented in Table 3. The calculated buckling capacities were compared with the forces in the stiffener from the characteristic loads (the special situation studied) in the discharging state (Tables 1 and Fig. 2). The largest resistance exceeding (35%) occurred within the strake 13 (third from bottom) in the area where there is a reduction in steel sheet thickness to 0.8 mm.

4. Numerical simulations

In order to assess the buckling capacity of the silo wall, numerical simulations were carried out using Linear Buckling Analysis (LBA) with the Symulia Abaqus software. This software was successfully used to perform LBA of thin walled beams as it was confirmed in [18].

The model accounted for the actual shape, appropriate thicknesses, and material properties of the corrugated sheets and stiffeners, as well as the shell construction of the hopper and roof, along with the bottom ring and column structure, according to the design documentation. Connections between the shell sheets and the stiffeners were modeled using pin-like, rigid sleeves placed at the bolt connection points, maintaining the appropriate distance between the median surfaces of the corrugated sheets and stiffeners (see Fig. 6).

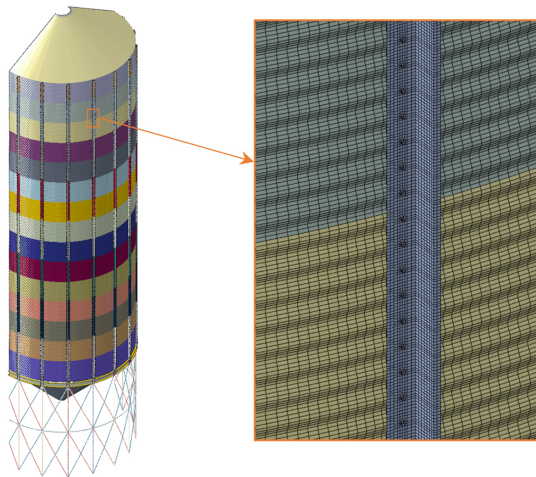


Fig. 6. Discrete model of the analysed silo section

For the purpose of the buckling analysis, details of the structural continuity of the stiffeners along their length were not included in the model. Utilizing the symmetry of the entire structure, only half of it was modeled.

The analysis considered characteristic loads in the discharging state, including tangential and normal pressures applied to the cylindrical wall of the silo. Additionally, it took into account hopper loads, the structure's self-weight, and loads from the supports of the charging gallery.

The conducted analysis showed that the examined silo has a buckling load capacity reserve. The smallest load multiplier for the characteristic applied loads was 2.35. The buckling mode involved the waviness of the silo wall, primarily in the area of corrugated sheet No. 11, along with corresponding waviness of the stiffeners. The form of stiffener waviness in this area involved cross-sectional torsion and is shown in Fig. 7b. Eighteen half-waves were noted around the entire circumference of the silo (see Fig. 7c), with a length equal to the circumferential distance between the stiffeners (see Fig. 7b). Vertically, ten half-waves were distinguished within the range of corrugated sheets 9–13 (see Fig. 7d), where the thickness of the corrugated sheets was 0.8 mm.

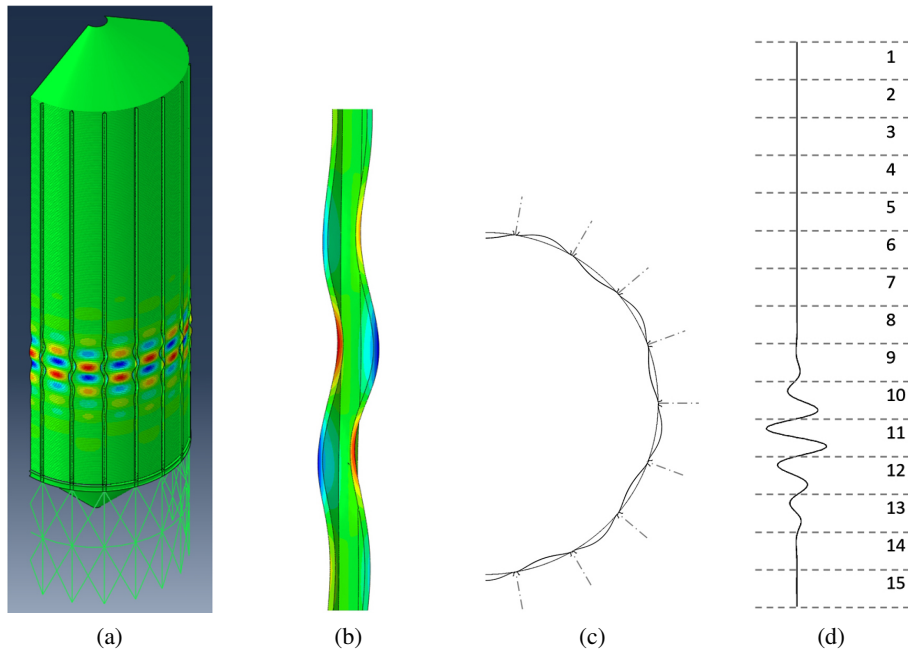


Fig. 7. Buckling mode for minimum load multiplier $\lambda = 2.35$: (a) considered section of the silo; (b) view of the stiffener buckling form; (c) waviness at the perimeter; (d) waviness diagram at the height of the cylindrical part of the silo

Subsequent buckling modes, associated with larger load multipliers, took on similar shapes and occurred at various heights of the silo.

5. Conclusions

The estimation of the buckling capacity of the silo wall using standard procedures led to two contrasting conclusions. The first method recommended by standard [15] indicated a reserve capacity. This result was obtained using the procedure appropriate for orthotropic walls with a stiffener spacing less than $d_{s,\min}$, even though this condition was not met. The resulting stability assessment of the silo wall could only be considered as a rough estimate.

The second method recommended by standard [16] showed insufficient buckling capacity of the wall for the characteristic loads during silo discharging. The maximum exceedance of the resistance reached 35%.

The numerical simulations performed, which accounted for both components of the load from the stored grain, confirmed the existence of a reserve buckling capacity of the silo wall. The minimum load multiplier for the characteristic load values was 2.35, and the buckling mode involved the waviness of the silo wall in the area of corrugated sheet No. 11.

The conducted numerical simulations confirmed a sufficient reserve capacity, as evidenced by the stable behavior of the structure under both grain storage and silo discharging conditions.

The presented calculations do not exhaust all analyses necessary to determine whether the silo discussed in this work can be safely operated. Separate groups of necessary verification calculations include the analysis of the bolt connections used in this silo, as well as the calculations for the hopper and columns supporting the entire silo. These analyses were beyond the scope of this presented work.

References

- [1] K. Rejowski and P. Iwicki, "Simplified stability analysis of steel cylindrical silos with corrugated walls and vertical columns", in *Recent Progress in Steel and Composite Structures*, Giżejowski, et al., Eds. Leiden: CRC Press/Balkema, 2016, pp. 525–532.
- [2] P. Iwicki, K. Rejowski, and J. Tejchman, "Simplified numerical model for global stability of corrugated silos with vertical stiffeners", *Journal of Constructional Steel Research*, vol. 138, pp. 93–116, 2017, doi: [10.1016/j.jcsr.2017.06.031](https://doi.org/10.1016/j.jcsr.2017.06.031).
- [3] P. Iwicki, K. Rejowski, and J. Tejchman, "Determination of buckling strength of silos composed of corrugated walls and thin-walled columns using simplified wall segment models", *Thin-Walled Structures*, vol. 135, pp. 414–436, 2019, doi: [10.1016/j.tws.2018.11.018](https://doi.org/10.1016/j.tws.2018.11.018).
- [4] E. Hotała, M. Kuśnierek, T. Kulczycki, and T. Wójcik, "Strefa przejściowa jako słabe miejsce płaszczu silosu z blachy falistej z fartuchem podporowym", in *Awarie budowlane: zapobieganie, diagnostyka, naprawy, rekonstrukcje*. Szczecin: Zachodniopomorski Uniwersytet Techniczny, 2017, pp. 659–668.
- [5] E. Hotała, Ł. Skotny, M. Kuśnierek, and J. Boniecka, "Experimental investigations on the resistance of vertical stiffeners of steel silos shells made of corrugated sheets", in *Recent Progress in Steel and Composite Structures*, Giżejowski, et al., Eds. Leiden: CRC Press/Balkema, 2016, pp. 186–187.
- [6] E. Hotała and M. Kuśnierek, "Nośność południkowych żeber płaszczu silosów z blachy falistej", *Materiały Budowlane*, no. 5, pp. 93–94, 2016.
- [7] E. Hotała, M. Kuśnierek, Ł. Skotny, and J. Boniecka, "Wadliwe połączenia żeber przyczyną awarii stalowych silosów o płaszczach z blach falistych", in *XXVII Konferencja Naukowo-Techniczna. Awarie Budowlane*. Szczecin: Zachodniopomorski Uniwersytet Techniczny, 2015, pp. 501–508.
- [8] E. Hotała, "Stalowe silosy na produkty rolne – rozwiązania konstrukcyjne, analizy nośności, trwałość, awarie", in *Budownictwo na obszarach wiejskich: nauka, praktyka, perspektywy*, A. Halicka, Ed. Lublin: Politechnika Lubelska, 2013, pp. 231–243.
- [9] P. Błażejowski and J. Marcinowski, "Nośność wyboconeniowa żeber wzmacniających ściany stalowego silosu na zboże", *Budownictwo i Architektura*, vol. 12, no. 2, pp. 189–196, 2013.
- [10] E. Hotała, *Stalowe silosy na produkty rolne – rozwiązania konstrukcyjne, analizy nośności, trwałość, awarie*. Lublin: Politechnika Lubelska, 2013, pp. 231–243.
- [11] E. Hotała and Ł. Skotny, "Stateczność walcowych płaszczu silosów stalowych uźebrowanych nad podporami odcinkowymi", *Przegląd Budowlany*, no. 6, pp. 119–122, 2012.
- [12] M. Wójcik, P. Iwicki, and J. Tejchman, "Analiza nośności wyboconeniowej cylindrycznego silosu z blachy falistej wzmocnionego słupami", *Inżynieria i Budownictwo*, no. 2, pp. 96–100, 2011.
- [13] P. Iwicki, M. Wójcik, and J. Tejchman, "Failure of cylindrical steel silos composed of corrugated sheets and columns and repair method using sensitivity analysis", *Engineering Failure Analysis*, vol. 18, no. 8, pp. 2064–2083, 2011, doi: [10.1016/j.engfailanal.2011.06.013](https://doi.org/10.1016/j.engfailanal.2011.06.013).
- [14] J. Marcinowski, "Flexural buckling resistance of stiffeners reinforcing wall of a steel silo," *Civil and Environmental Engineering Reports*, vol. 33, no. 3, pp. 89–98, 2023, doi: [10.59440/ceer/176939](https://doi.org/10.59440/ceer/176939).
- [15] PN-EN 1993-4-1: 2009 Eurokod 3. Projektowanie konstrukcji stalowych. Część 4-1: Silosy. PKN, 2009.
- [16] PN-EN 1993-4-1:2009/A1:2017-08 Amendment A1 to: Eurocode 3. Design of steel structures. Part 4-1: Silos. PKN, 2017 (in Polish).

- [17] PN-EN 1991-4: 2006 Eurokod 1. Oddziaływania na konstrukcje. Część 4: Silosy i zbiorniki. PKN, 2006.
- [18] PN-EN 1993-1-1: 2006 Eurokod 3. Projektowanie konstrukcji stalowych. Część 1-1: Reguły ogólne i reguły dla budynków. PKN, 2006.

Nośność wyboczeniowa ściany stalowego silosu na zboże

Słowa kluczowe: blacha falista, żebra ścienne, obliczenia analityczne, silos stalowy, symulacje numeryczne, nośność wyboczeniowa

Streszczenie:

Ściany stalowych silosów na zboże są narażone na utratę stateczności. Przyczyną tego niepożądanego zjawiska są pionowe oddziaływania zboża składowanego w silosie na ściany najczęściej wykonywane z blachy falistej o poziomym układzie fal. Siły te wywołane tarcieniem materiału magazynowanego o ścianę, są tym większe im większa jest chropowatość ściany. Zewnętrzne żebra pionowe wzmacniają ścianę silosu i wraz z blachą falistą tworzą powłokową strukturę ortotropową. Procedury zawarte w obowiązujących normach umożliwiają oszacowanie nośności wyboczeniowej ściany tak skonstruowanego silosu. W pracy przedstawiono przykład analizy nośności wyboczeniowej ściany silosu stalowego o pojemności 700 m³. Zastosowano dwie spośród metod zalecanych w obowiązujących normach. Wykonano także symulacje numeryczne, których celem było określenie krytycznego poziomu intensywności obciążenia. Przeprowadzone analizy pozwoliły wyciągnąć wnioski dotyczące nośności wyboczeniowej ściany analizowanego silosu.

Received: 2024-09-15, Revised: 2024-10-21